INTERNATIONAL JOURNAL FOR NUMERICAL METHODS IN ENGINEERING
Int. J. Numer. Meth. Engng 2001; **51**:159–179

Numerical study of grid distribution effect on accuracy of DQ analysis of beams and plates by error estimation of derivative approximation

C. Shu[1,*,†], W. Chen[1], H. Xue[1] and H. Du[2]

[1] *Department of Mechanical and Production Engineering, National University of Singapore, 10 Kent Ridge Crescent, Singapore 119260, Singapore*
[2] *School of Mechanical and Production Engineering, Nanyang Technological University, Nanyang Avenue, Singapore 2263, Singapore*

SUMMARY

The accuracy of global methods such as the differential quadrature (DQ) approach is usually sensitive to the grid point distribution. This paper is to numerically study the effect of grid point distribution on the accuracy of DQ solution for beams and plates. It was found that the stretching of grid towards the boundary can improve the accuracy of DQ solution, especially for coarse meshes. The optimal grid point distribution (corresponding to optimal stretching parameter) depends on the order of derivatives in the boundary condition and the number of grid points used. The optimal grid distribution may not be from the roots of orthogonal polynomials. This differs somewhat from the conventional analysis. This paper also proposes a simple and effective formulation for stretching the grid towards the boundary. The error distribution of derivative approximation is also studied, and used to analyze the effect of grid point distribution on accuracy of numerical solutions. Copyright © 2001 John Wiley & Sons, Ltd.

KEY WORDS: differential quadrature; grid structure; truncation error; high-order boundary value problems

1. INTRODUCTION

The differential quadrature (DQ) method was originally introduced by Bellaman and his associates [1] as a simple and highly efficient numerical technique. One essential issue pertaining to the method is how to determine its weighting coefficients efficiently and accurately. The earlier approach, which requires solving algebraic equations with an ill-conditioned Vandermonde matrix, is neither efficient nor accurate when the number of grid points is large [1, 2]. Based on the Lagrange interpolation, Quan and Chang [3] provided explicit formulations to compute the weighting coefficients of the DQ discretization of the first and second order

*Correspondence to: C. Shu, Department of Mechanical and Production Engineering, National University of Singapore, 10 Kent Ridge Crescent, Singapore 119260, Singapore
†E-mail: mpeshuc@nus.edu.sg

Received 25 June 1999
Revised 28 June 2000

derivatives. More generally, Shu [4], Shu and Richards [5] presented the generalized differential quadrature (GDQ) method, in which the determination of weighting coefficients of the DQ discretization is generalized under the analysis of a high-order polynomial approximation and the analysis of a linear vector space. A simple formulation was given for computing the weighting coefficients of the first-order derivative with arbitrary mesh point distribution, and the weighting coefficients of the second and higher order derivatives are computed by a recurrence formulation. The mathematical fundamentals and recent developments of the DQ method as well as its major applications in engineering are discussed in detail in the book of Shu [6].

As shown in the book of Shu [6], DQ is a global method, which is equivalent to the highest-order finite-difference scheme. As compared to the low-order finite-difference schemes and finite element methods, the DQ method can obtain very accurate numerical results by using a considerably small number of grid points. Consequently, it requires much less computational effort and virtual storage. In general, the DQ method uses a non-uniform mesh for numerical discretization. It was shown [3, 7] that for many problems, the use of non-uniform meshes resulting from the roots of orthogonal polynomials is very efficient. However, in the application of the DQ method to the free vibrational analysis of plates with free corner conditions, Shu and Du [8] found that the mesh points given from orthogonal polynomials could not yield accurate and reliable solutions. A further stretching of mesh points to the boundary is necessary to guarantee the accuracy and convergence in the computation of these cases. The work recognized the limitation of the traditional choice of grid points and a new way to determine the grid points was provided [8]. It is well known that the grid point distribution plays an essential role in determining the accuracy, convergence speed and stability of the DQ method. However, a major shortcoming of the method is just the lack of adequate studies to evaluate convergence with regard to grid spacing and grid structure [9]. Quan and Chang [10] compared numerically the performances of the often-used non-uniform meshes and concluded that the grid points originated from the Chebyshev polynomials of the first kind is optimum in all cases examined there. Bert and Malik [7] indicated an important fact that the preferred type of grid points changes with problems of interest and recommended the use of Chebyshev–Gauss–Lobatto grid for structural mechanics computation. Moradi and Taheri [11] also investigated the effect of various spacing schemes on the accuracy of DQ results for buckling application of composites. They provided insight into the influence of a number of sampling points in conjunction to various spacing schemes. All the above work has not provided sensible explanations why certain type of grid points is superior to the others in the computation of their problems. Only one explicit conclusion reached their work is that the selection of non-uniform mesh from the roots of orthogonal polynomials or functions can greatly enhance the accuracy of the quadrature solution in comparison to uniform mesh. Chen [9] also identified the limitation of conventional non-uniform meshes for analysing of the second- and fourth-order differential systems. However, as pointed out by Bert and Malik [7], the issue of the proper choice of the grid points remains largely an unclear matter. All above trigger the present work.

The objective of this paper is to systematically study the relationship between the spacing of grid points and errors of DQ results for bending and vibration analysis of beams and plates with various boundary conditions. The stretching function given by Shu [6] will be adopted in the present study. It was found that the stretching of conventional grid points is very useful to improve the accuracy of DQ results, especially when using the small number of grid points. In terms of accuracy, it was found that for each case, there exists an optimal grid point distribution, which corresponds to the optimal stretching parameter. Since in the DQ method, the coordinates of grid points are used to construct the approximated polynomial, the optimal mesh point distribution corresponds to the optimal polynomial approximation. Our systematic numerical experiments showed that for most cases of vibration and bending problems, the optimal grid points are not from the roots of orthogonal polynomials. In other words, the orthogonal polynomials may not be the best approximation to a boundary value problem. This differs somewhat from the conventional analysis. The effect of grid stretching on the accuracy of numerical results was systematically studied by the error distribution of derivative approximation using the newly developed formulations of Chen [9]. It is believed that this paper presents some significant guidelines to properly choose the grid points in the DQ computation of structural mechanics problems.

2. DQ METHOD AND ERROR ANALYSIS

The essence of the differential quadrature method is that the partial derivative of a function with respect to a variable is approximated by a weighted sum of function values at all discrete points in that direction. Its weighting coefficients are not related to any special problem and only depend on the grid spacing. Thus, any partial differential equation can be easily reduced to a set of algebraic equations using these coefficients. Considering a function $f(x)$ with N grid points, we have

$$\left.\frac{\partial^m f(x)}{\partial x^m}\right|_{x_i} = \sum_{j=1}^{N} c_{ij}^{(m)} f(x_j), \quad i = 1, 2, \ldots, N \tag{1}$$

where x_j are the co-ordinates of grid points in the variable domain. $f(x_j)$ and $c_{ij}^{(m)}$ are the function values at grid points and the related weighting coefficients, respectively. Based on the analysis of a linear vector space, Shu and Richards [5] developed the GDQ method to generalize all the ways to compute the weighting coefficients in DQ approximation. For the first-order derivative, the weighting coefficients are computed as

$$c_{ij}^{(1)} = \frac{1}{x_j - x_i} \prod_{\substack{k=1 \\ k \neq i,j}}^{N} \frac{x_i - x_k}{x_j - x_k}, \quad i = 1, 2, \ldots, N; \; j = 1, 2, \ldots, N, \; i \neq j \tag{2a}$$

and

$$c_{ii}^{(1)} = -\sum_{j \neq i}^{N} c_{ij}^{(1)}, \quad i = 1, 2, \ldots, N \tag{2b}$$

For the second- and higher-order derivatives, the weighting coefficients can be generated by the following recurrent formulation [5]:

$$c_{ij}^{(m+1)} = m\left(c_{ij}^{(1)} c_{ii}^{(m)} - \frac{c_{ij}^{(m)}}{x_i - x_j}\right), \quad i \neq j \tag{3a}$$

and

$$c_{ii}^{(m+1)} = -\sum_{j \neq i}^{N} c_{ij}^{(m+1)} \tag{3b}$$

where the superscript (m) and $(m+1)$ denote the order of derivatives. The details of the method and its applications can be found in Reference [6].

The DQ method can be derived by Lagrangian interpolated polynomial. Let function $f(x)$ be smooth enough, the Lagrangian interpolated polynomial can be written as

$$f(x)=\sum_{j=1}^{N} p_j(x)f(x_j)+R(x), \quad j=1,2,\ldots,N \tag{4}$$

where $p_j(x)$ are Lagrangian interpolated polynomials, $R(x)$ is the truncation error given by

$$R(x)=\frac{f^{(N)}(\xi)W(x)}{N!} \tag{5}$$

Here $W(x)=\prod_{i=1}^{N}(x-x_i)$. Differentiating Equation (4) with respect to x, we can obtain

$$f^{(1)}(x_i)=\sum_{j=1}^{N} p_j^{(1)}(x_i)f(x_j)+R^{(1)}(x_i)=\sum_{j=1}^{N} c_{ij}^{(1)}f(x_j)+R^{(1)}(x_i) \tag{6}$$

where $c_{ij}^{(1)}$ are the DQ weighting coefficients of the first order derivative, x_i denote the coordinates of grid points, $R^{(1)}(x_i)$ is the truncation error of the first-order derivative approximation by the DQ method at the grid point x_i

$$R^{(1)}(x_i)=\frac{f^{(N)}(\xi)W^{(1)}(x_i)}{N!}, \quad i=1,2,\ldots,N \tag{7}$$

where ξ is an unknown function of variable x. Setting

$$|W^{(1)}(x_i)|=\left|\prod_{k\neq i}^{N}(x_i-x_k)\right|=p(x_i), \quad e^{(1)}(x_i)=\frac{p(x_i)}{N!} \quad \text{and} \quad K_1=\max\{|f^{(N)}(\xi)|\}$$

then we have

$$R^{(1)}(x_i)\leqslant K_1\frac{|W^{(1)}(x_i)|}{N!}=K_1\frac{p(x_i)}{N!}=K_1e^{(1)}(x_i), \quad i=1,2,\ldots,N \tag{8}$$

For the second-order derivative, we can have

$$R^{(2)}(x_i)=\frac{2\xi_x f^{(N+1)}(\xi)W^{(1)}(x_i)}{N!}+\frac{f^{(N)}(\xi)W^{(2)}(x_i)}{N!}, \quad i=1,2,\ldots,N \tag{9}$$

Using the DQ approach, we have the following relationship [6]:

$$c_{ii}^{(m-1)}=\frac{W^{(m)}(x_i)}{mW^{(1)}(x_i)} \tag{10}$$

where $c_{ii}^{(m-1)}$ are the diagonal entries of the DQ weighting coefficient matrix for the $(m-1)$th-order derivative. $W^{(m)}$ denotes the mth order derivative of the function $W(x)$. Equation (10) can be rewritten as

$$W^{(m)}(x_i)=mc_{ii}^{(m-1)}W^{(1)}(x_i) \tag{11}$$

Substituting Equation (11) into Equation (9), we have

$$|R^{(2)}(x_i)|\leqslant 2K_2\left(1+\left|c_{ii}^{(1)}\right|\right)\frac{p(x_i)}{N!}=K_2e^{(2)}(x_i) \tag{12}$$

where $K_2 = \max\{|f^{(N)}(\xi)|, |\xi_x f^{(N+1)}(\xi)|\}$, $e^{(2)}(x_i)$ is the error coefficients of the second-order derivative. Similarly, we can obtain

$$|R^{(3)}(x_i)| \leqslant 3K_3 \left(2 + \left|c_{ii}^{(1)}\right| + \left|c_{ii}^{(2)}\right|\right) \frac{p(x_i)}{N!} = K_3 e^{(3)}(x_i) \tag{13}$$

$$|R^{(4)}(x_i)| \leqslant 4K_4 \left(5 + 6\left|c_{ii}^{(1)}\right| + 3\left|c_{ii}^{(2)}\right| + \left|c_{ii}^{(3)}\right|\right) \frac{p(x_i)}{N!} = K_4 e^{(4)}(x_i) \tag{14}$$

for truncation errors of the third- and fourth-order derivative, respectively, where K_3 and K_4 are the maximum values of composite derivatives of ξ and $f(x)$ up to $(N+3)$ order, and $e^{(3)}(x_i)$ and $e^{(4)}(x_i)$ are the corresponding error coefficients. The above error estimates are different from those given by Bellman [1] in that they can analyze the truncation error at every grid point.

3. GOVERNING EQUATIONS AND NUMERICAL DISCRETIZATION

The first application of differential quadrature method to solve problems in structural mechanics was given by Bert *et al.* [12]. Since then, the method has been applied successfully to a wide range of structural mechanics problems (see Reference [7] and references therein). The two essential points in these applications are how to select grid points and how to apply double boundary conditions at each edge of physical domain. The second issue has attracted considerable attention in recent years [7–9, 12–17]. Shu and Du [8, 17] provided persuasive evidences that the most simple, efficient and flexible approach is to directly implement double boundary conditions at each boundary point. Shu and Du's approach is generally successful and has no limitation for its use. In this study, the approach of Shu and Du [8, 17] is adopted to implement the two conditions at the boundary point. The numerical examples are the bending and vibration of beams and plates with various boundary conditions. The analysis of these problems has been done in many references [7–9, 11–17] for showing the advantages of the DQ method over the other numerical techniques or for comparisons among various approaches applying multiple boundary conditions. The major contribution of this paper is to provide some innovations on how to choose grid points in the DQ method rather than new numerical case studies. In order to simplify presentation, SS, C and F represent simply-supported, clamped and free edges, respectively. The plates of various configurations are denoted by the respective boundary conditions. For example, an SS–C–SS–F rectangular plate would have simply supported edges at $x=0$ and $x=1$, clamped edge at $y=0$, and free edge at $y=1$.

3.1. Transverse bending and vibration of beams

For the case of a Bernoulli–Euler beam with Length L, the governing equation of deflection and vibration is given by

$$\frac{d^2}{dx^2}\left(EI\frac{d^2 w}{dx^2}\right) = -q(x) - m\frac{d^2 w}{dt^2} \tag{15}$$

where E, I, q, and m are the elastic module, area moment of inertia about the neutral axis, distributed lateral loading, and mass per unit length, respectively. In this study, EI and m are assumed constants, $q(x) = q_0 \sin(x\pi/L)$. Let $X = x/L$, the analog governing equations in terms of the DQ discretization at interior points can be written as

$$\sum_{j=1}^{N} c_{ij}^{(4)} w_j = -\frac{L^4 q_0}{EI} \sin(\pi X), \quad i = 3, \ldots, N-2 \tag{16}$$

for deflection, and

$$\sum_{j=1}^{N} c_{ij}^{(4)} w_j = \varpi^2 w_i, \quad i = 3, \ldots, N-2 \tag{17}$$

for vibration, where $c_{ij}^{(4)}$ are the weighting coefficients of the fourth-order derivative, w_j is the deflection at point x_j, $\varpi^2 = mL^4\omega^2/EI$ is the normalized frequency, ω is the natural frequency of free vibration. The boundary conditions are given as follows:

Clamped end:

$$w = 0, \quad w_{,X} = 0 \quad \text{at } X = 0, 1 \tag{18a}$$

In terms of DQ discretization, Equation (18a) can be reduced to

$$w_1 = 0, \quad \sum_{j=1}^{N} c_{1j}^{(1)} w_j = 0; \quad w_N = 0, \quad \sum_{j=1}^{N} c_{Nj}^{(1)} w_j = 0 \tag{18b}$$

Simply supported end:

$$w = 0, \quad w_{,XX} = 0 \quad \text{at } X = 0, 1 \tag{19a}$$

The DQ analog equations of Equation (19a) can be written as

$$w_1 = 0, \quad \sum_{j=1}^{N} c_{1j}^{(2)} w_j = 0; \quad w_N = 0, \quad \sum_{j=1}^{N} c_{Nj}^{(2)} w_j = 0 \tag{19b}$$

Free end:

$$w_{,XX} = 0, \quad w_{,XXX} = 0 \quad \text{at } X = 0, 1 \tag{20}$$

The DQ discretization equations of Equation (20) are

$$\sum_{j=1}^{N} c_{1j}^{(2)} w_j = 0, \quad \sum_{j=1}^{N} c_{1j}^{(3)} w_j = 0, \quad \text{at } X = 0 \tag{21a}$$

$$\sum_{j=1}^{N} c_{Nj}^{(2)} w_j = 0, \quad \sum_{j=1}^{N} c_{Nj}^{(3)} w_j = 0, \quad \text{at } X = 1. \tag{21b}$$

For a detailed implementation of the above boundary conditions, the work of Shu and Du [8] can be referred to. It is to be noted that at each end, there are two boundary conditions. So, in total, there are four boundary condition equations. For a well-posed problem, the number of equations must be equal to the number of unknowns. Therefore, the discrete governing equation (16) or (17) has to be applied at $(N-4)$ interior points. This can be done by applying these equations at the points x_i, $i = 3, 4, \ldots, N-2$.

3.2. Transverse vibration of thin, isotropic rectangular plates

The non-dimensional equation governing free vibration of rectangular plates can be expressed as

$$w_{,xxxx} + 2\lambda^2 w_{,xxyy} + \lambda^4 w_{,yyyy} = \varpi^2 w \tag{22}$$

where $\lambda = a/b$ is the aspect ratio, $\varpi^2 = \rho h a^4 \omega^2 / D$, D denotes the plate stiffness, h represents the total plate thickness, and ρ stands for the density, w and ω are the model deflection and the natural frequency of free vibration. Equation (22) can be discretized by the DQ method as

$$\sum_{k=1}^{N} c_{ik}^{(4)} w_{kj} + (2\lambda^2)\sum_{k=1}^{N}\sum_{m=1}^{M} c_{ik}^{(2)}\,\bar{c}_{jm}^{(2)} w_{km} + (\lambda^4)\sum_{k=1}^{M} \bar{c}_{jk}^{(4)} w_{ik} = \varpi^2 w_{ij} \quad i = 3,\ldots,N-2, \quad j = 3,\ldots,M-2 \tag{23}$$

where $c_{ik}^{(2)}, \bar{c}_{jm}^{(2)}$, $c_{ik}^{(4)}$ and $\bar{c}_{jk}^{(4)}$ represent the DQ weighting coefficients of the second and fourth-order derivatives along x- and y-direction, respectively. The following boundary conditions will be considered in the present study.

Clamped edge:

$$w = 0, \quad w_{,x} = 0 \quad \text{at } x = 0, 1 \tag{24a}$$

$$w = 0, \quad w_{,y} = 0 \quad \text{at } y = 0, 1 \tag{24b}$$

Simply supported edge:

$$w = 0, \quad w_{,xx} = 0 \quad \text{at } x = 0, 1 \tag{25a}$$

$$w = 0, \quad w_{,yy} = 0 \quad \text{at } y = 0, 1 \tag{25b}$$

Free edge:

$$w_{,xx} + v\lambda^2 w_{,yy} = 0, \quad w_{,xxx} + (2-v)\lambda^2 w_{,xyy} = 0 \quad \text{at } x = 0, 1 \tag{26a}$$

$$\lambda^2 w_{,yy} + v w_{,xx} = 0, \quad \lambda^2 w_{,yyy} + (2-v) w_{,xxy} = 0 \quad \text{at } y = 0, 1 \tag{26b}$$

At the free corner, the boundary condition is

$$w_{,xy} = 0 \tag{27}$$

In this study, the approach of Shu and Du [17] is applied to implement the above boundary conditions.

3.3. Transverse vibration of thin, isotropic skew plates

The configuration of a skew plate is shown in Figure 1. The non-dimensional differential equation for small-amplitude flexural vibration of a thin, isotropic, skew plate can be written as

$$w_{,xxxx} - 4\lambda\cos\theta w_{,xxxy} + 2\lambda^2(1 + 2\cos^2\theta) w_{,xxyy} - 4\lambda^3\cos\theta w_{,xyyy} + \lambda^4 w_{,yyyy} = \varpi^2 \sin^4\theta w \tag{28}$$

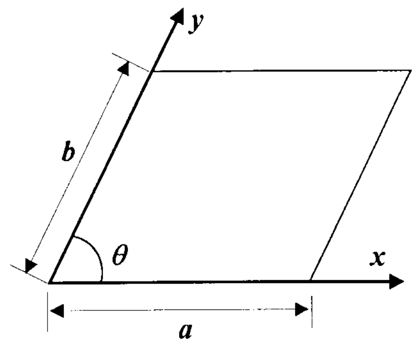

Figure 1. A skew plate.

where $\lambda = a/b$ is the aspect ratio, θ is the skew angle, $\varpi^2 = \rho h a^4 \omega^2 / D$. In this study, the clamped and simply supported conditions are considered, which are given as

Clamped edge:

$$w = 0, \quad w_{,x} = 0 \quad \text{at } x = 0, 1 \tag{29a}$$

$$w = 0, \quad w_{,y} = 0 \quad \text{at } y = 0, 1 \tag{29b}$$

Simply supported edge:

$$w = 0, \quad w_{,xx} - 2\cos\theta w_{,xy} = 0 \quad \text{at } x = 0, 1 \tag{30a}$$

$$w = 0, \quad w_{,yy} - 2\cos\theta w_{,xy} = 0 \quad \text{at } y = 0, 1 \tag{30b}$$

Similar to the rectangular plate, the governing equation (28) and boundary conditions (29) and (30) can be discretized by the DQ method, and the approach of Shu and Du [17] is applied to implement the boundary conditions.

4. TYPICAL GRIDS AND GRID STRETCHING

The five typical grids, which are commonly used in the literature, are considered in this study. The co-ordinates of grid points are supposed to be within the normalized domain $x \in [0, 1]$. In the following, N represents the number of grid points in each direction.

Type I: Equally spaced grid points:

$$x_i = \frac{i-1}{N-1}, \quad i = 1, 2, \ldots, N \tag{31}$$

Type II: Normalized grid points originated from the roots of Chebyshev polynomials of the second kind:

$$x_i = \frac{r_i - r_1}{r_N - r_1}, \quad i = 1, 2, \ldots, N \tag{32}$$

where $r_i = \cos i\pi/(N+1)$.

Type III: Normalized grid points originated from the roots of Legendre polynomials:

$$x_i = \frac{r_i - r_1}{r_N - r_1}, \quad i = 1, 2, \ldots, N \tag{33}$$

where

$$r_i = \left(1 - \frac{1}{8N^2} + \frac{1}{8N^3}\right) \cos \frac{4i - 1}{4N + 2} \pi$$

Type IV: Normalized grid points originated from the roots of Chebyshev polynomials of the first kind:

$$x_i = \frac{r_i - r_1}{r_N - r_1}, \quad i = 1, 2, \ldots, N \tag{34}$$

where

$$r_i = \cos \frac{(2i - 1)\pi}{2N}$$

Type V: Chebyshev-Gauss-Lobatto points (Lobatto points in short):

$$x_i = \frac{1}{2}\left(1 - \cos\left(\frac{i - 1}{N - 1}\pi\right)\right), \quad i = 1, 2, \ldots, N \tag{35}$$

Apart from the above five typical grids, in this study, we will further stretch the traditional grid points towards the boundary by using the following formulation [6]:

$$x_i = (1 - \alpha)(3\xi_i^2 - 2\xi_i^3) + \alpha\xi_i, \quad i = 1, 2, \ldots, N, \ \alpha \leqslant 1 \tag{36}$$

where α is the stretching parameter, ξ_i are the co-ordinates of the basic grid points. Obviously, the less the value of α, the stronger the grid points are stretched towards the boundary. It is noted that the stretching equation (36) can only be applied for the domain of $0 \leqslant \xi \leqslant 1$. After stretching by Equation (36), x is still in the domain of $0 \leqslant x \leqslant 1$. It is noted that when α is taken as a negative value, the obtained x_2 from Equation (36) may become a small negative value, which is outside of the domain [0, 1]. For this case, the co-ordinates of x_2 and x_{N-1} are given from the following formulation:

$$x_2 = \sigma x_3, \quad x_{N-1} = 1 - x_2 \tag{37}$$

where σ is a small positive constant. In general, the choice of σ follows the condition of $\Delta x_1 = x_2 - x_1 < \Delta x_2 = x_3 - x_2$. In the present study, σ is taken as 0.1, and the Lobatto points given by Equation (35) are adopted as the basic grid points since their distribution has the strongest tendency towards the boundary among the above-mentioned five grids. Clearly, when $\alpha = 1$, the stretched grid points are actually the original Lobatto grid points.

Table I displays the coordinates of grid points for the above five grids as well as a variety of the stretched Lobatto grids with $N = 9$. The parameter SI in Table I is the abbreviation of Stretching Index, which is defined as

$$\mathrm{SI} = \sum_{i=1}^{N/2} \bar{x}_i \Bigg/ \sum_{i=1}^{N/2} x_i \tag{38}$$

where $\bar{x}$ is the co-ordinate of the equally spaced points, x is the co-ordinate of other grid points. SI shows what extent the total distribution of grid points tends toward the boundary.

Table I. Co-ordinates of grid points for various grids ($N = 9$).

Grids	x_1	x_2	x_3	x_4	x_5	x_6	x_7	x_8	x_9	SI
Equ	0.0	0.125	0.25	0.375	0.5	0.625	0.75	0.875	1.0	1.0
Che II	0.0	0.075	0.191	0.338	0.5	0.662	0.809	0.925	1.0	1.24
Leg	0.0	0.068	0.183	0.333	0.5	0.667	0.817	0.932	1.0	1.28
Che I	0.0	0.060	0.174	0.326	0.5	0.674	0.826	0.940	1.0	1.34
Lob	0.0	0.038	0.146	0.308	0.5	0.691	0.853	0.962	1.0	1.52
$\alpha = 0.8$	0.0	0.031	0.129	0.292	0.5	0.708	0.871	0.969	1.0	1.55
$\alpha = 0.6$	0.0	0.025	0.111	0.276	0.5	0.724	0.889	0.975	1.0	1.59
$\alpha = 0.4$	0.0	0.018	0.093	0.260	0.5	0.740	0.907	0.982	1.0	1.64
$\alpha = 0.2$	0.0	0.011	0.076	0.243	0.5	0.757	0.924	0.989	1.0	1.70
$\alpha = 0.0$	0.0	0.004	0.058	0.227	0.5	0.773	0.942	0.996	1.0	1.78
$\alpha = -0.2$	0.0	0.004	0.040	0.211	0.5	0.789	0.960	0.996	1.0	1.84
$\alpha = -0.4$	0.0	0.002	0.023	0.194	0.5	0.806	0.977	0.998	1.0	1.92
$\alpha = -0.6$	0.0	0.0005	0.005	0.178	0.5	0.822	0.995	0.9995	1.0	2.11

The larger the value of SI, the closer the grid points towards the boundary. It can be seen from Table I that Lobatto grid (Type V) has the most evident tendency towards the boundary among the five typical grids. Following are Chebyshev grid of the first kind (Type IV), Legendre grid (Type III), and Chebyshev grid of the second kind (Type II). For simplicity, Chebyshev, Legendre and Lobatto are abbreviated as Che, Leg and Lob in all the tables.

5. NUMERICAL RESULTS AND DISCUSSIONS

The results presented in this section attempt to illustrate the effect of grid spacing on the numerical accuracy. For this purpose, the relative error or difference is defined as

$$e_k = \left| \frac{\text{DQ} - \text{Reference}}{\text{Reference}} \right| \tag{39}$$

where e_k indicates the relative error or difference of the deflection at the grid point x_k, in bending problems or the kth frequency in vibration problems. The average error or difference is defined by

$$\varepsilon = \frac{1}{L} \sum_{k=1}^{L} e_k \tag{40}$$

For the following discussion, optimal stretching parameter is defined as the one with which the average relative error is minimized.

5.1. Bending of beams

A varying load

$$q = q_0 \sin(\pi x / L) \tag{41}$$

is applied for this problem. At first, we study the effect of various grid point distributions on the accuracy of DQ results. It was found that the stretched Lobatto grid points with proper value of α usually produce more accurate DQ results for all cases in comparison to

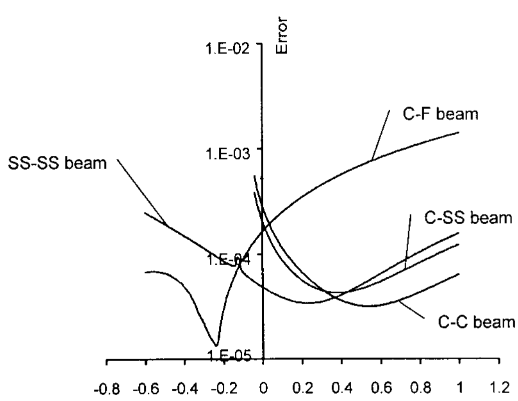

Figure 2. Average error of deflection versus α for various beams ($N=9$).

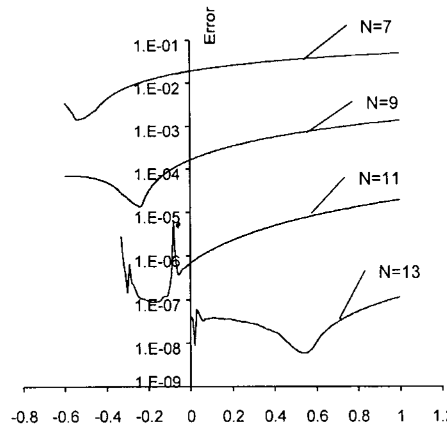

Figure 3. Average error of deflection versus α for C–F beam by using different number of grid points.

the conventional non-uniform grids, and the optimal grid spacing varies with the boundary condition of the problem. In general, the grid points are required to be more stretched to the boundary in order to obtain accurate solutions for problems with boundary conditions of higher order derivatives. For example, when $N=9$, the optimal stretching parameter is $\alpha=-0.2$ for the C−F beam, and $\alpha=0.6$ for the C−C beam. This feature can be observed from Figure 2. The reason is possibly due to the fact that the former boundary conditions involve the second and third order derivatives, while the latter only involves the first order derivative. We will further discuss this issue in the analysis of error distribution for derivative approximation.

On the other hand, it was found that as the number of grid points increases, the optimal stretching parameter also increases. This can be seen clearly in Figure 3, which shows the average error of deflection versus α for C−F beam with different numbers of grid points. It is clearly observed from Figure 3 that the optimal stretching parameter α increases as the number of grid points goes up. It is noted that Lobatto grid is a stretching grid towards the boundary. The stretching of Lobatto grid will be enhanced as the number of grid points increases. The results in Figure 3 show that, to obtain accurate DQ solutions, Lobatto grid is not stretched enough for coarse meshes. So, for small value of N, we need to use small value of α to get accurate DQ results. As N increases, the optimal value of α will be increased up to $\alpha=1$. This phenomenon can also be seen in Table II and Figure 4. Table II lists the minimized average errors in conjunction with the optimal stretching parameter α for different number of mesh points, while Figure 4 illustrates the convergence behavior of different grids for SS−SS beam. It can be seen from Table II that for the coarse mesh, the stretching of grid is necessary to obtain accurate DQ solutions. When the number of grid points is increased to above 13, the optimal grid for C−C, C−SS and SS−SS beams is the Chebyshev grid of the second kind, which has the least tendency towards the boundary among all non-uniform grids listed in Table I. It seems that the grid with smaller stretching tendency is more suitable when

Table II. Minimized average error of DQ results for bending of beams under varying load of $q = q_0 \sin(\pi x/L)$.

N	7	9	11	13	15
C–C	1.53E−3 ($\alpha = 0.53$)	3.18E−5 ($\alpha = 0.54$)	1.74E−6 (Che II)	2.42E−6 (Che II)	3.40E−6 (Che II)
C–SS	7.92E−4 ($\alpha = 0.26$)	4.30E−5 ($\alpha = 0.38$)	2.56E−6 (Che I)	1.63E−6 (Che II)	2.26E−6 (Che II)
SS–SS	2.77E−4 ($\alpha = 0.22$)	3.39E−5 ($\alpha = 0.23$)	3.46E−7 ($\alpha = 0.47$)	2.19E−7 (Che II)	2.06E−7 (Che II)
C–F	1.46E−3 ($\alpha = -0.54$)	1.33E−5 ($\alpha = -0.24$)	8.98E−8 ($\alpha = -0.17$)	5.89E−9 ($\alpha = 0.54$)	4.40E−8 (Lob)

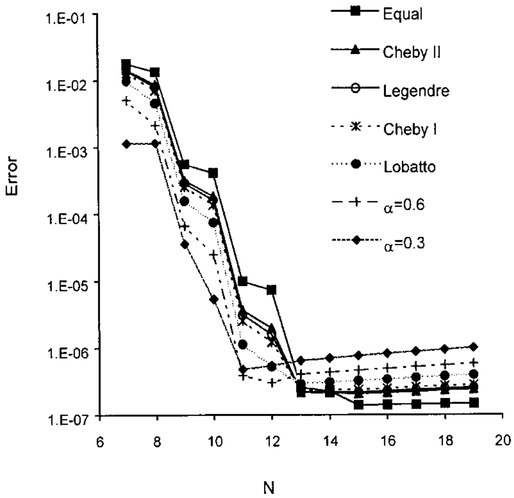

Figure 4. Average error of deflection versus N for SS–SS beam using different grids.

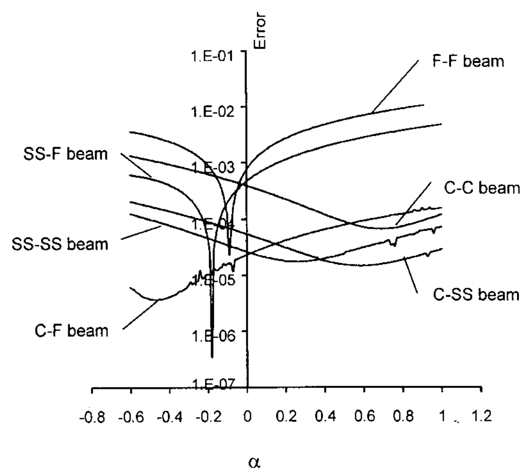

Figure 5. Relative error of fundamental frequency versus α for various beams ($N = 9$).

$N \geqslant 13$. From Figure 4, we can see that the optimal convergence could be achieved with the stretched grid of $\alpha = 0.3$ when $N \leqslant 13$. As N is further increased to above 13, the traditional grids give better accuracy than the stretched Lobatto grids.

5.2. Vibration of beams

The vibration of beams with various combinations of SS, C and F boundary conditions was also investigated. It was found that the accuracy of DQ solution depends on the grid. The stretched Lobatto grid with proper choice of α provides much more accurate solutions than the traditional non-uniform grids in all the cases examined. Like the bending problem, the optimal stretching parameter also depends on the boundary condition. As the order of derivative in the boundary conditions increases, the optimal stretching parameter α declines and the

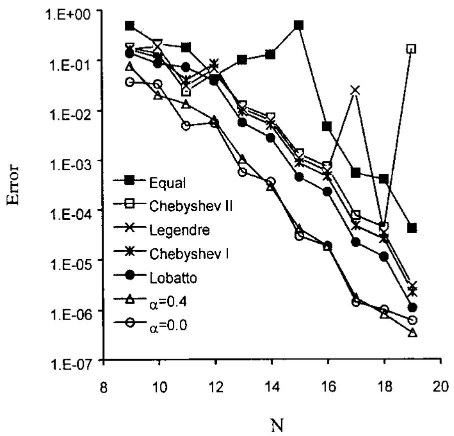

Figure 6. Average error of the first three frequencies versus N for F–F beam using different grids.

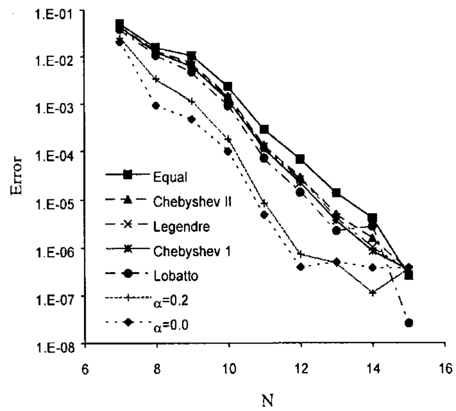

Figure 7. Relative error of fundamental frequency versus N for SS–F beam using different grids.

corresponding stretching towards the boundary is enhanced. This can be observed in Figure 5, which displays the error of fundamental frequency versus α for various combinations of boundary conditions with $N=9$. The reference data in this study are given by Blevin [19]. It is seen that there exists a best grid for each case, and the DQ method can yield very accurate results with the stretched grid points as small as $N=9$. It is interesting to see from Figure 5 that for the SS−F and F−F beams, the α-error curve is very sharp in the vicinity of optimal stretching parameter. The accuracy of DQ results can be greatly improved within a small range of α. It may be concluded that the DQ solution is very sensitive to the grid for these cases. In contrast, the remaining curves for C−C, C−SS, SS−SS and C−F beams are somehow smooth.

In order to obtain an accurate numerical solution, it was found that the SS−F and F−F beams require the strongest stretching towards the boundary (lowest value of α) among all test examples. The converging tendency of various grids in the DQ solutions of SS−F and F−F beams are revealed in Figures 6 and 7, respectively. Clearly, the accuracy of DQ solution depends on the grid. It is observed that the stretched Lobatto grid points have the most rapid converging speed in both figures. For small value of N, the DQ solutions with the stretched Lobatto grids are much more accurate than those with the conventional non-uniform grids. It can be seen from Figure 6 that the solutions using equally spaced points, Legendre points and Chebyshev II points oscillate obviously. This means that the traditional non-uniform grids are not reliable in the DQ solution of vibrational problems. As shown in Figures 6 and 7, the grid of $\alpha=0.0$ renders the best solutions, while the equally spaced grid yields the worst ones. The original Lobatto grid performs the best among the five conventional grids for all cases.

5.3. Vibration of isotropic rectangular plates

The results for vibration of square plates with all edges free, clamped or simply supported are presented in Table III. The relative errors listed in the table are obtained in terms of the Leissa's solution [18]. Like the beams, the stretched Lobatto grid points can generate accurate

Table III. Relative errors of numerical frequencies for square plates using different grids.

	Errors of fundamental frequency $N=M=9$			Average errors of the first five frequencies $N=M=13$		
Grids	C–C–C–C	SS–SS–SS–SS	F–F–F–F	C–C–C–C	SS–SS–SS–SS	F–F–F–F
Equ	1.02E−3	1.31E−4	2.76E−1	1.20E−1	6.65E−1	2.30E−1
Che II	5.90E−4	7.63E−5	2.20E−1	3.49E−4	3.09E−4	1.83E−1
Leg	5.24E−4	6.71E−5	2.10E−1	2.96E−4	2.47E−4	1.71E−1
Che I	4.41E−4	5.84E−5	1.97E−1	*2.47E−4*	1.89E−4	1.52E−1
Lob	1.82E−4	3.56E−5	1.56E−1	2.61E−4	8.02E−5	1.06E−1
$\alpha=0.8$	5.24E−5	2.63E−5	1.17E−1	3.04E−4	4.33E−5	6.25E−2
$\alpha=0.6$	*7.76E−6*	1.66E−5	8.17E−2	3.38E−4	1.44E−5	3.39E−2
$\alpha=0.4$	5.90E−5	*1.02E−5*	5.07E−2	3.75E−4	*5.28E−6*	1.55E−2
$\alpha=0.2$	2.40E−4	1.20E−5	2.59E−2	4.47E−4	4.03E−5	4.78E−3
$\alpha=0.0$	1.96E−4	1.54E−5	8.98E−3	2.16E−3	5.25E−5	*6.50E−4*
$\alpha=-0.2$	7.01E−3	2.89E−5	*2.98E−4*	4.21E−2	9.81E−5	3.84E−3
$\alpha=-0.4$	2.91E−2	4.39E−5	6.55E−3	6.24E−2	1.55E−4	3.42E−2
$\alpha=-0.6$	1.51E−2	1.50E−4	1.20E−2	1.18E−1	2.20E−4	2.73E−2

Table IV. Relative errors of the first five frequencies for SS–F–F–F rectangular plates ($N=M=11$, $\alpha_x=\alpha_y=-0.1$).

$\lambda=a/b$	e_1 (%)	e_2 (%)	e_3 (%)	e_4 (%)	e_5 (%)	ε (%)
0.4	0.09	0.52	0.10	0.66	0.69	0.41
2/3	0.07	0.52	0.66	0.59	0.07	0.39
1	0.06	0.82	0.44	0.49	0.53	0.47
1.5	0.05	0.86	0.35	0.70	0.51	0.49
2.5	0.80	0.04	0.74	0.27	0.38	0.46

DQ solutions for plates. In general, the accuracy of stretched Lobatto grid is about one- or two-order higher than the traditional non-uniform grids. However, there is one exception, that is, the plate with all edges clamped. For this case, the average relative error of the first five frequencies is minimized by using Chebyshev I grid when $N=13$. This is because the clamped condition only involves the first-order derivative in the boundary condition and the number of grid points is large, which requires less stretching to the boundary. This is especially true when N is large. On the other hand, it is noted that only stretched Lobatto grid points can yield reliable solutions for F−F−F−F plates with free corners. For the case without any free corner, it was found that the conventional Lobatto grid can also generate accurate results.

When the plate has at least one free corner, the conventional five grids cannot generate any meaningful solution. This has been highlighted by Shu and Du [17]. In this work, more cases with free corners are studied. The relative percentage differences of the first five frequencies between the DQ solutions and the results of Leissa [18] are listed in Table IV for SS−F−F−F plate. For this case, the stretched Lobatto grid with $\alpha_x=\alpha_y=-0.1$ is used and different aspect ratios of 0.4, 2/3, 1, 1.5, 2.5 are considered. The optimal choice of $\alpha_x=\alpha_y=-0.1$ is through the trial and error process due to the difficulty of rigorous mathematical analysis. In the later section, we will try to analyze this problem through the error distribution of derivative approximation.

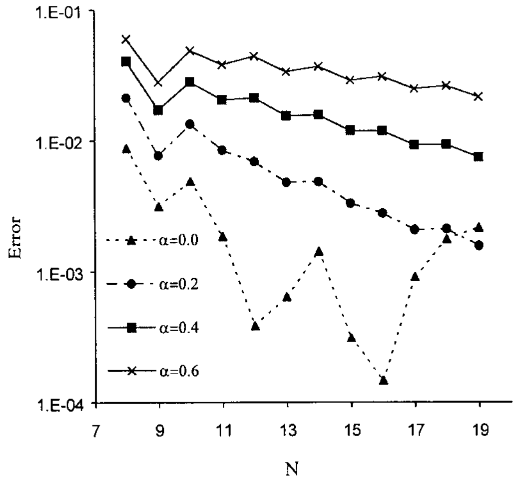

Figure 8. Average error of the first five frequencies versus N for F–F–F–F square plates using different grids.

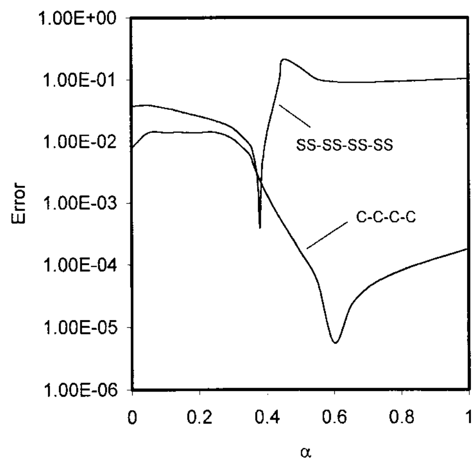

Figure 9. Relative error of fundamental frequency versus α for a skew plate of $a=b$, $\theta=45°$ ($N=15$).

Figure 8 compares the accuracy of DQ solution with the stretched grids of $\alpha=0, 0.2, 0.4, 0.6$ for completely free square plate. In each case, the type and number of grid points are taken the same in both the x and y directions. The average relative differences of the first five frequencies between the DQ solution and the reference data of Leissa and Narita [20] are displayed. The differences are plotted against the number of grid points for each grid. The traditional non-uniform grids resulted from the orthogonal polynomials do not work well for this case, and, thus, are not included in the figure. Figure 8 shows that the grid of $\alpha=0$ gives more accurate results than the other three grids. However, the curve shows high oscillation. When N is large, the DQ solution of this case does not show any convergence trend. In contrast, the solutions of other grids have obvious convergence trend. Among the four grids, the grid of $\alpha=0.6$ generates the least accurate DQ solution. Although the convergence tendency is shown for this grid, the convergence is so slow that the solutions do not converge to reasonable accuracy even up to $N=19$. The convergence rate can be greatly enhanced by selecting a smaller value of α.

5.4. Vibration of isotropic skew plates

The stretched Lobatto grid is used to study the effect of grid spacing on the accuracy of DQ solutions for vibration analysis of skew plates with all edges clamped or simply supported. For simplicity, we only show the results for the case of $a=b$. The stretching parameter α is taken the same in the x and y direction, respectively. It was found that for the simply supported case, the accuracy of the fundamental frequency is lower than other low-order frequencies, and is very sensitive to the grid when θ is less than 75°. In contrast, for the clamped case, the accuracy of fundamental frequency remains the same order as other low-order frequencies, and is less sensitive to the skew angle θ. When the same number of grid points is used, the clamped results are more accurate than the simply supported results. For any given angle of θ and plate configuration, there is an optimal grid (optimal stretching

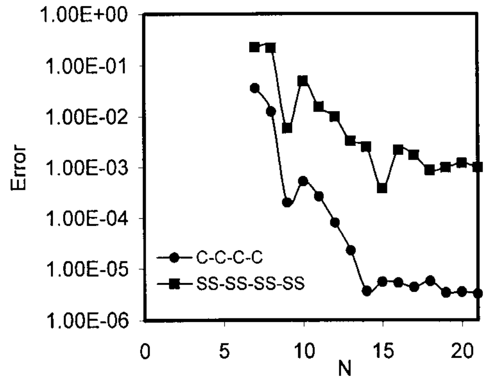

Figure 10. Relative error of fundamental frequency versus N for a skew plate of $a=b$, $\theta=45°$.

parameter α) in terms of the accuracy of numerical results. In general, the optimal stretching parameter for the clamped case is larger than that for the simply supported case. This can be seen clearly from Figure 9, which shows the error of fundamental frequency versus α for simply supported and clamped conditions and $N=15$, $\theta=45°$. The reference data used in this study are given from the work of Liew and Lam [21]. We can see from Figure 9 that the optimal stretching parameter is around 0.38 for the simply supported condition and 0.6 for the clamped condition. This means that, to obtain accurate DQ results, the clamped configuration requires less stretching towards the boundary than the simply supported configuration. This conclusion is in line with that drawn from the studies of beams and rectangular plates. The reason is probably due to the approximation of derivatives in the boundary conditions. As we know, the clamped condition only involves the first-order derivative while the simply supported condition involves the second-order derivatives. As will be shown in the following section, the DQ approximation of the first-order derivative is much more accurate than the second-order derivative. It can also be observed from Figure 9 that the accuracy of DQ results for the clamped condition is much higher than that for the simply supported condition, and the DQ results of SS–SS–SS–SS skew plates are very sensitive to the grid (α value). Like the vibration of SS–F and F–F beams, the α-error curve of SS–SS–SS–SS skew plates is very sharp in the vicinity of optimal stretching parameter. On the other hand, it was found that as N (the number of grid points) increases, the accuracy of DQ results is improved with proper choice of α. However, when N is above a certain value, the accuracy of DQ results cannot be further improved. This phenomenon can be seen in Figure 10, which shows the relative error of fundamental frequency versus N for simply supported and clamped conditions and $\theta=45°$. For the results shown in Figure 10, the stretching parameter is taken as 0.6 for the clamped condition, and 0.38 for the simply supported condition.

5.5. Analysis by error distribution of derivative approximation

In this part, the error distribution of derivative approximation for the grids given in Table I is studied by using the formulation given in Section 2. The coefficients of error distribution for the respective derivatives only depend on the coordinate of grid points. The distribution of grid points determines the distribution of truncation error for derivative approximation.

Table V. Error coefficients of DQ approximation for the first-order derivative ($N=9$).

Grids	x_1	x_2	x_3	x_4	x_5	ε
Equ	6.6E−9	8.3E−10	2.4E−10	1.2E−10	9.5E−11	1.7E−9
Che II	3.3E−9	9.1E−10	4.8E−10	3.5E−10	3.1E−10	1.2E−9
Leg	2.9E−9	8.9E−10	5.2E−10	3.9E−10	3.6E−10	1.1E−9
Che I	2.5E−9	8.6E−10	5.6E−10	4.6E−10	4.3E−10	1.0E−9
Lob	1.3E−9	6.7E−10	6.7E−10	6.7E−10	6.7E−10	8.2E−10
$\alpha=0.8$	9.7E−10	5.3E−10	6.6E−10	8.2E−10	9.0E−10	7.6E−10
$\alpha=0.6$	6.5E−10	3.9E−10	6.2E−10	9.8E−10	1.2E−9	7.2E−10
$\alpha=0.4$	3.9E−10	2.6E−10	5.6E−10	1.2E−9	1.5E−9	7.0E−10
$\alpha=0.2$	1.9E−10	1.5E−10	4.7E−10	1.3E−9	2.0E−9	6.9E−10
$\alpha=0.0$	5.6E−11	4.9E−11	3.6E−10	1.5E−9	2.5E−9	7.1E−10
$\alpha=-0.2$	3.6E−11	3.1E−11	2.0E−10	1.6E−9	3.0E−9	7.4E−10
$\alpha=-0.4$	1.1E−11	9.5E−12	7.5E−11	1.7E−9	3.5E−9	8.0E−10
$\alpha=-0.6$	5.1E−12	4.5E−12	4.3E−12	1.7E−9	4.4E−9	8.7E−10

Therefore, the error estimate is useful to provide some insights into the analysis of the results presented in the previous parts, in which the effect of grid distribution on the DQ solution is investigated in detail. It is certain that the accuracy of DQ solutions is dependent on the error distribution of derivatives involved in problems of interest. In the present study, the approach of implementing the multiple boundary conditions proposed by Shu and Du [17] is adopted. For this approach, the discretized governing equations at points immediately adjacent to the boundary are replaced by the discretized derivative boundary condition equations. Thus, the truncation errors of discretized governing equations at these points have no effect on the accuracy of numerical solutions. In other words, there is no need to consider the truncation errors of discretized governing equations at these points. Therefore, the major concerns are how to accurately approximate the boundary conditions at the boundary points and the governing equations at other interior points. Analysis of the magnitude and the distribution of estimated errors may clarify what factor leads to significant improvement of DQ resolutions in applying the stretched Lobatto grids.

The absolute error coefficients of the first-, second-, third- and fourth-order derivatives for grids shown in Table I are listed in Tables V, VI, VII and VIII, respectively. Due to the symmetry of grid points used, the error coefficients are only shown in the range of [0, 0.5]. In general, the error coefficients at the same grid point are much larger for high-order derivatives than for lower-order derivatives. It is also noted that the truncation error coefficients unevenly distribute and are closely related to the grid point distribution. For the traditional uniform and non-uniform grids, larger error coefficients locate at the boundary points. These grids also have a feature that the error coefficients of all derivatives are gradually decreased from the boundary point to the centre point. When the grid is stretched towards the boundary, the error coefficients at the points near the boundary will be decreased while the error coefficients at the points near the centre of the domain will be increased. When the stretching of grid is properly chosen, the error coefficients will be uniformly distributed. For this case, accurate numerical results can be expected. It was found from the tables that the error coefficients of the original Lobatto grid are distributed more uniformly than other four conventional grids. This could be the reason that the Lobatto grid generally yields the most accurate DQ solution in comparison to the other four conventional grids.

Table VI. Error coefficients of DQ approximation for the second-order derivative ($N=9$).

Grids	x_1	x_2	x_3	x_4	x_5	ε
Equ	3.0E−7	2.3E−8	4.1E−9	1.1E−9	1.9E−10	7.3E−8
Che II	1.9E−7	1.4E−8	3.4E−9	1.4E−9	6.3E−10	4.7E−8
Leg	1.8E−7	1.1E−8	3.0E−9	1.3E−9	7.2E−10	4.4E−8
Che I	1.6E−7	7.5E−9	2.3E−9	1.3E−9	8.6E−10	3.9E−8
Lob	1.2E−7	9.8E−9	3.2E−9	1.9E−9	1.3E−9	3.0E−8
$\alpha=0.8$	9.8E−8	1.3E−8	6.3E−9	4.1E−9	1.8E−9	2.7E−8
$\alpha=0.6$	7.9E−8	1.5E−8	9.6E−9	6.9E−9	2.4E−9	2.5E−8
$\alpha=0.4$	6.1E−8	1.8E−8	1.3E−8	1.0E−8	3.1E−9	2.3E−8
$\alpha=0.2$	4.5E−8	1.9E−8	1.5E−8	1.4E−8	3.9E−9	2.1E−8
$\alpha=0.0$	3.0E−8	2.1E−8	1.7E−8	1.9E−8	4.9E−9	2.0E−8
$\alpha=-0.2$	2.0E−8	1.3E−8	1.6E−8	2.3E−8	6.0E−9	1.7E−8
$\alpha=-0.4$	1.1E−8	7.2E−9	1.2E−8	2.8E−8	7.3E−9	1.4E−8
$\alpha=-0.6$	2.2E−9	1.6E−9	3.5E−9	3.3E−8	8.7E−9	1.0E−8

Table VII. Error coefficients of DQ approximation for the third-order derivative ($N=9$).

Grids	x_1	x_2	x_3	x_4	x_5	ε
Equ	8.4E−6	7.2E−8	9.6E−8	6.3E−8	5.2E−8	1.9E−6
Che II	6.3E−6	6.9E−7	2.4E−7	1.4E−7	1.1E−7	1.7E−6
Leg	6.1E−6	8.0E−7	2.7E−7	1.5E−7	1.2E−7	1.6E−6
Che I	5.7E−6	9.7E−7	2.9E−7	1.6E−7	1.4E−7	1.6E−6
Lob	4.8E−6	1.6E−6	3.8E−7	2.2E−7	1.8E−7	1.6E−6
$\alpha=0.8$	4.3E−6	1.7E−6	4.2E−7	2.5E−7	2.2E−7	1.5E−6
$\alpha=0.6$	3.8E−6	1.8E−6	4.4E−7	2.9E−7	2.6E−7	1.4E−6
$\alpha=0.4$	3.3E−6	1.9E−6	4.2E−7	3.2E−7	3.0E−7	1.4E−6
$\alpha=0.2$	2.8E−6	2.0E−6	3.6E−7	3.5E−7	3.5E−7	1.3E−6
$\alpha=0.0$	2.4E−6	2.0E−6	2.2E−7	3.6E−7	4.1E−7	1.2E−6
$\alpha=-0.2$	2.0E−6	1.7E−6	1.5E−7	3.5E−7	4.6E−7	1.0E−6
$\alpha=-0.4$	1.7E−6	1.5E−6	5.1E−7	3.3E−7	5.3E−7	9.5E−7
$\alpha=-0.6$	1.3E−6	1.3E−6	1.0E−6	2.9E−7	6.0E−7	9.2E−7

For the stretched Lobatto grid, the stretching extent depends on the value of α in the stretching formulation (36). For example, the stretched grid with $\alpha=0.0$ has more tendency towards the boundary than that with $\alpha=0.8$. As the stretching is enhanced, the error coefficients will be decreased at points near the boundary and, inversely, increased at points near the central region. It can be seen clearly that when the stretching parameter α is less than 0.8 for the first-order derivative (Table V), and less than 0.0 for the second-order derivative (Table VI), the value of error coefficients at the boundary point is even less than that at the central point. Although in the stretched Lobatto grids, the error coefficients for the third- and fourth-order derivatives at boundary points always remain larger than those at the central point, the relative differences are reduced obviously when the grid is stretched. This information implies that as the grid is stretched towards the boundary, the approximation of derivatives in the boundary condition is improved. Therefore, the accuracy of DQ solution is improved when the Lobatto grid is further stretched. The information also hints that the DQ approximation at the boundary point is not accurate enough in the traditional non-uniform grids including

Table VIII. Error coefficients of DQ approximation for the fourth-order derivative ($N = 9$).

Grids	x_1	x_2	x_3	x_4	x_5	ε
Equ	1.7E−4	1.3E−5	3.7E−6	1.1E−6	2.1E−7	4.2E−5
Che II	1.4E−4	3.4E−5	5.0E−6	1.4E−6	4.4E−7	4.1E−5
Leg	1.4E−4	3.8E−5	5.0E−6	1.4E−6	4.8E−7	4.1E−5
Che I	1.3E−4	4.3E−5	4.9E−6	1.4E−6	5.4E−7	4.1E−5
Lob	1.2E−4	5.9E−5	3.9E−6	1.3E−6	7.2E−7	4.1E−5
$\alpha = 0.8$	1.1E−4	6.3E−5	2.1E−6	1.3E−6	8.6E−7	4.1E−5
$\alpha = 0.6$	1.1E−4	6.6E−5	4.2E−6	2.2E−6	1.0E−6	4.0E−5
$\alpha = 0.4$	9.9E−5	7.0E−5	8.1E−6	3.3E−6	1.2E−6	4.0E−5
$\alpha = 0.2$	9.1E−5	7.3E−5	1.3E−5	4.6E−6	1.4E−6	4.0E−5
$\alpha = 0.0$	8.3E−5	7.6E−5	1.9E−5	5.9E−6	1.6E−6	4.1E−5
$\alpha = -0.2$	7.5E−5	7.1E−5	2.8E−5	7.3E−6	1.8E−6	4.1E−5
$\alpha = -0.4$	7.0E−5	6.7E−5	4.1E−5	8.7E−6	2.1E−6	4.2E−5
$\alpha = -0.6$	6.3E−5	6.3E−5	5.6E−5	1.0E−5	2.4E−6	4.3E−5

the original Lobatto grid. On the other hand, it has been found in the numerical experiments that the stretching cannot be overly done. When stretching parameter α in Equation (36) is too small, the errors resulting from the DQ discretization of governing equation at interior points may become predominant to make the solution worse. An inappropriate stretching, overly or too weakly, may not exhibit the deliberate balance of truncation errors between the discretized boundary conditions at the boundary point and the discretized governing equations at the interior points.

As discussed earlier on, the improvement of accuracy of DQ results may be due to the improvement of derivative approximation in the boundary condition equations. We can see clearly from Tables V–VIII that the accuracy of the first-order derivative approximation can be greatly improved when the grid is slightly stretched. In contrast, the improvement of the second-order derivative approximation requires stronger stretching (smaller value of α) of the grid. The improvement for the approximation of the third and fourth-order derivatives is much slower than that for the approximation of the first- and second-order derivatives. This means that much stronger stretching (very small value of α) is needed to improve the approximation of the third- and fourth-order derivatives. Since the clamped boundary condition equation only involves the first-order derivative, a slight stretching of the grid can generate accurate DQ results. As the simply supported and free boundary condition equations involve the second- and third-order derivatives, a stronger stretching of the grid is needed to improve the accuracy of DQ results. This analysis is in line with the founding of numerical examples as shown previously.

6. CONCLUSIONS

This paper studied the effect of grid point distribution on the DQ solution of structural mechanics problems. It was found that the non-uniform grids from the roots of orthogonal polynomials such as the Legendre, Lobatto, and Chebyshev grids can generally provide accurate numerical solutions. However, these grids are not always optimal with respect to the solution accuracy vis-à-vis the number of grid points. This is particularly true when the coarse mesh is used and the problems with high-order derivatives in the boundary condition are considered. For most cases, the original Lobatto grid is the best choice among the four traditional non-uniform grids. The stretched Lobatto grid with proper choice of stretching parameter can improve the accuracy of numerical solution. The stretching is especially efficient for coarse meshes. For some cases such as problems with free corners, the stretching is necessary to obtain reliable solutions. The choice of optimal stretching parameter depends on the order of derivative in the boundary condition and the number of grid points used. The stretching of grid cannot be excessively employed, since an inappropriate stretching may not balance the truncation errors between the discretized boundary conditions at the boundary point and the discretized governing equations at the interior points.

Mathematically, it is known that for a given boundary value problem, there exists an optimal polynomial which is the best approximation to the solution of the problem. However, it is very difficult to find such a polynomial by analytical tools. The present work can be considered to numerically find the optimal polynomial approximation for a given boundary value problem. In terms of accuracy, it was found that for each case, there exists an optimal grid point distribution, which corresponds to the optimal stretching parameter. Since in the DQ method, the coordinates of grid points are used to construct the approximated polynomial, the optimal grid point distribution corresponds to the optimal polynomial approximation. Our systematic studies showed that for most cases of vibration and bending problems, the optimal grid points are not from the roots of orthogonal polynomials. In other words, the orthogonal polynomials may not be the best approximation to a boundary value problem. This observation has also been highlighted in the work of Moradi and Taheri [11].

REFERENCES

1. Bellman RE, Kashef BG, Casti J. Differential quadrature: a technique for the rapid solution of nonlinear partial differential equations. *Journal of Computational Physics* 1972; **10**:40–52.
2. Civan F, Sliepcevich CM. Differential quadrature for multidimensional problems. *Journal of Mathematical Analysis and Applications* 1984; **101**:423–443.
3. Quan JR, Chang CT. New insights in solving distributed system equations by the quadrature methods—I. *Computers in Chemical Engineering* 1989; **13**:779–788.
4. Shu C. Generalized differential-integral quadrature and application to the simulation of incompressible viscous flows including parallel computations. *Ph.D. Dissertation*, University of Glasgow, UK, 1991.
5. Shu C, Richards BE. Parallel simulation of incompressible viscous flows by generalized differential quadrature. *Computing Systems Engineering* 1992; **3**:271–281.
6. Shu C. *Differential Quadrature and its Application in Engineering*. Springer: Berlin, January 2000.
7. Bert CW, Malik M. Differential quadrature method in computational mechanics: a review. *Applied Mechanical Reviews* 1996; **49**:1–28.
8. Shu C, Du H. A generalized approach for implementing general boundary conditions in the GDQ free vibration analysis of plates. *International Journal of Solids and Structures* 1997; **34**:837–846.
9. Chen W. Differential quadrature method and its applications in engineering. *Ph.D. Dissertation*, Shanghai Jiao Tong University, China, 1996.
10. Quan JR, Chang CT. New insights in solving distributed system equations by the quadrature methods—II. *Computers in Chemical Engineering* 1989; **13**:1017–1024.
11. Moradi S, Taheri F. Differential quadrature approach for delamination buckling analysis of composites with shear deformation. *AIAA Journal* 1998; **36**:1869–1873.
12. Bert CW, Jang SK, Striz AG. Two new methods for analyzing free vibration of structural components. *AIAA Journal* 1988; **26**:612–618.
13. Wang X, Bert CW. A new approach in applying differential quadrature to static and free vibrational analyses of beams and plates. *Journal of Sound and Vibration* 1993; **62**:566–572.
14. Malik M, Bert CW. Implementing multiple boundary conditions in the DQ solution of higher-order PDE's: application to free vibration of plates. *International Journal for Numerical Methods in Engineering* 1996; **39**:1237–1258.

15. Wang X, Gu H. Static analysis of frame structures by the differential quadrature element method. *International Journal for Numerical Methods in Engineering* 1997; **40**:759–772.
16. Chen W, Striz AG, Bert CW. A new approach to the differential quadrature method for quadrature method for fourth-order equations. *International Journal for Numerical Methods in Engineering* 1997; **40**:1941–1956.
17. Shu C, Du H. Implementation of clamped and simply supported boundary conditions in the GDQ free vibration analysis of beams and plates. *International Journal of Solids and Structures* 1997; **34**:819–835.
18. Leissa W. The free vibration of rectangular plates. *Journal of Sound and Vibration* 1973; **31**:257–293.
19. Blevins D. *Formulas for Natural Frequency and Mode Shape*. Robert E. Krieger: Malabar, FL, 1984.
20. Leissa W, Narita Y. Vibration of completely free shallow shells of rectangular platform. *Journal of Sound and Vibration* 1984; **96**:207–218.
21. Liew KM, Lam KY. Application of two-dimensional orthogonal plate function to flexural vibration of skew plates. *Journal of Sound and Vibration* 1990; **139**:241–252.

